Estimates of the spectral aerosol single scattering albedo and aerosol radiative effects during SAFARI 2000

Robert W. Bergstrom,[1] Peter Pilewskie,[2] Beat Schmid,[1] and Philip B. Russell[2]

Received 9 April 2002; revised 5 August 2002; accepted 2 October 2002; published 18 February 2003.

[1] Using measurements of the spectral solar radiative flux and optical depth for 2 days (24 August and 6 September 2000) during the SAFARI 2000 intensive field experiment and a detailed radiative transfer model, we estimate the spectral single scattering albedo of the aerosol layer. The single scattering albedo is similar on the 2 days even though the optical depth for the aerosol layer was quite different. The aerosol single scattering albedo was between 0.85 and 0.90 at 350 nm, decreasing to 0.6 in the near infrared. The magnitude and decrease with wavelength of the single scattering albedo are consistent with the absorption properties of small black carbon particles. We estimate the uncertainty in the single scattering albedo due to the uncertainty in the measured fractional absorption and optical depths. The uncertainty in the single scattering albedo is significantly less on the high-optical-depth day (6 September) than on the low-optical-depth day (24 August). On the high-optical-depth day, the uncertainty in the single scattering albedo is 0.02 in the midvisible whereas on the low-optical-depth day the uncertainty is 0.08 in the midvisible. On both days, the uncertainty becomes larger in the near infrared. We compute the radiative effect of the aerosol by comparing calculations with and without the aerosol. The effect at the top of the atmosphere (TOA) is to cool the atmosphere by 13 W m^{-2} on 24 August and 17 W m^{-2} on 6 September. The effect on the downward flux at the surface is a reduction of 57 W m^{-2} on 24 August and 200 W m^{-2} on 6 September. The aerosol effect on the downward flux at the surface is in good agreement with the results reported from the Indian Ocean Experiment (INDOEX). *INDEX TERMS:* 0305 Atmospheric Composition and Structure: Aerosols and particles (0345, 4801); 0345 Atmospheric Composition and Structure: Pollution—urban and regional (0305); 0360 Atmospheric Composition and Structure: Transmission and scattering of radiation; 3359 Meteorology and Atmospheric Dynamics: Radiative processes; 3360 Meteorology and Atmospheric Dynamics: Remote sensing; *KEYWORDS:* aerosols, absorption, black carbon, biomass burning

Citation: Bergstrom, R. W., P. Pilewskie, B. Schmid, P. B. Russell, Estimates of the spectral aerosol single scattering albedo and aerosol radiative effects during SAFARI 2000, *J. Geophys. Res.*, *108*(D13), 8474, doi:10.1029/2002JD002435, 2003.

1. Introduction

[2] The aerosol effects on atmospheric radiation remain a major uncertainty in understanding past and present climates and in predicting the future climate. Recent scientific research planning documents [*Ramanathan et al.*, 2002, available at http://www-nacip.ucsd.edu] emphasize the importance of absorbing aerosol components in directly affecting Earth-atmosphere radiation budgets and in determining aerosol-cloud interactions. Particles with no absorption have a negative (cooling) forcing while particles with substantial absorption can have a positive (warming) forcing. Simple calculations show that a small amount of strongly absorbing particles such as black carbon can change a negative aerosol forcing to a positive aerosol forcing. Aerosol absorption also deposits solar energy that would have warmed Earth's surface into atmospheric layers aloft. There it can shorten cloud lifetimes by causing them to "burn off" [*Ackerman et al.*, 2000].

[3] Determining the absorption of solar radiation by aerosols in the atmosphere is quite difficult. One can either infer the single scattering albedo from in situ measurements of aerosol light scattering and absorption or from the inversion of radiometric measurements. However, recent sensitivity studies have shown a significant difference among various in situ and radiometric determinations of the single scattering albedo [*Russell et al.*, 2002]. Consequently, there is a fair amount of uncertainty associated with aerosol absorption and the aerosol single scattering albedo [*Heintzenberg et al.*, 1997].

[4] The dry season component of the Southern African Regional Science Initiative (SAFARI 2000) was conducted during August and September 2000 in Southern Africa [see *Swap et al.*, 2002]. A major objective of the experiment was the study of the smoke aerosol generated from biomass burning. Biomass burning produces significant amounts of aerosol including absorbing black carbon particles [*Reid and Hobbs*, 1998].

[1]Bay Area Environmental Research Institute, Sonoma, California, USA.
[2]NASA Ames Research Center, Moffett Field, California, USA.

0148-0227/03/2002JD002435$09.00

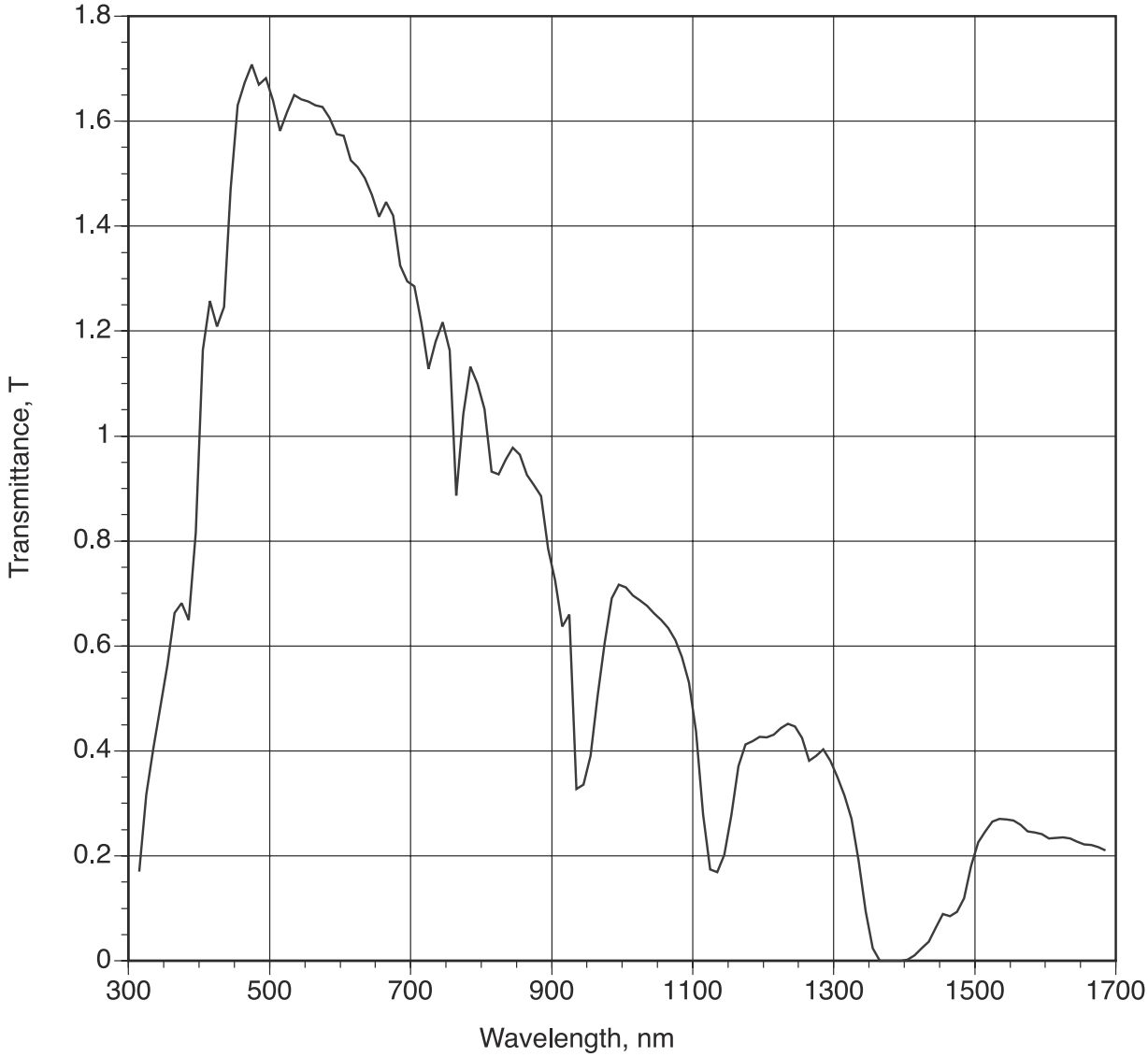

Figure 1. Transmitted beam at the surface, midlatitude summer, $\mu_0 = 1.0$.

[5] *Bergstrom et al.* [2002] recently discussed the solar absorption properties of black carbon particles. They indicated that, in general, the single scattering albedo of a mixture of black carbon and other nonabsorbing aerosols should decrease with wavelength. This is in contrast to many mineral dusts that have a single scattering albedo that increases with wavelength.

[6] During SAFARI 2000 the NASA Ames Solar Spectral Flux Radiometer (SSFR) and 14 channel Ames Airborne Tracking Sun Photometer (AATS-14) were deployed on the University of Washington Convair-580 [*Sinha et al.*, 2003, Appendix]. The SSFR made simultaneous measurements of upwelling and downwelling solar spectral irradiance while the AATS-14 measured the optical depth of the atmosphere above the aircraft. The Convair-580 profiled the lower troposphere, thus providing measurements above, in and below the aerosol layers.

[7] The spectral radiative flux measurements made by the SSFR during SAFARI 2000 are presented in more detail in a companion paper of *Pilewskie et al.* [2003]. The SSFR is a moderate resolution flux (irradiance) spectrometer covering the wavelength range from 300 to 1700 nm. The absolute accuracy of SSFR irradiance spectra depends mostly on the accuracy of the transfer standard. The uncertainty over the spectral range was between 1% and 3%. An additional error occurs during aircraft operations because of aircraft pitch and roll. Corrections are applied to the downwelling flux to correct for these effects.

[8] *Pilewskie et al.* [2003] present measurements of the flux divergence (absorption) and fractional absorption for the aerosol layer on 2 days of SAFARI 2000; 24 August 2000 and 6 September 2000. They show that although the aerosol optical depths for the 2 days are significantly different, the absorption efficiency (absorption per unit optical depth) was quite similar.

[9] The aerosol optical depth and water vapor profiles were measured by the NASA Ames airborne Sun photometer as discussed in detail by *Schmid et al.* [2003]. The AATS-14 measures the transmission of the direct solar beam in 14 spectral channels (0.354 to 1.557 μm). The Sun photometer tracks the Sun so that the detectors are kept normal to the solar beam as the aircraft changes orientation.

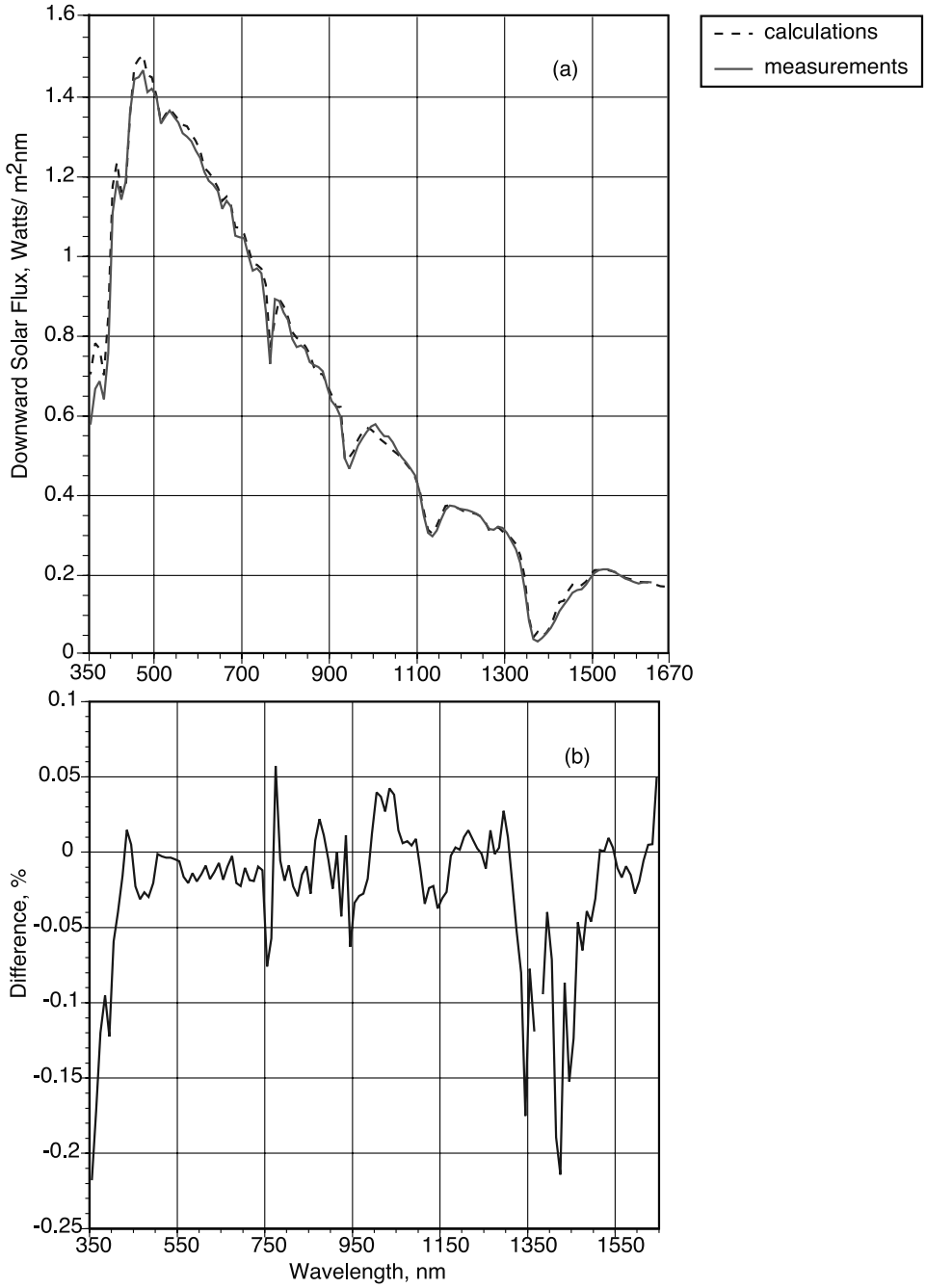

Figure 2. 24 August: Measured and calculated downward flux (a), difference, in percent, between measured and calculated values shown in Figure 2a (b), $\mu_0 = 0.80$.

[10] The calibration of the airborne Sun photometer is determined via Langley plots at remote mountaintop locations. The aerosol optical depth is retrieved at 13 narrow wavelength intervals as is the columnar amount of water vapor. The uncertainty estimates are presented in some detail by *Schmid et al.* [2003]. For this study, we used an uncertainty of 0.02 in the optical depth.

[11] The purpose of this paper is to estimate the spectral aerosol single scattering albedo and radiative effects during SAFARI 2000. Specifically, we take the measured spectral solar radiative fluxes and the aerosol optical depth above and below the aerosol layer and using a radiative transfer model estimate the aerosol single scattering albedo and its uncertainty. We present results for 2 days, 24 August and 6 September 2000. We then use the determined aerosol properties to estimate the effect of the aerosol on the solar radiation by simply comparing the calculations with and without the aerosol.

2. Radiative Transfer Model

[12] We have developed a numerical radiative transfer model specifically for analysis of the SSFR data. The major features of the model include the following:

1. *k*-distribution representation for O_2, O_3, CO_2, and H_2O absorption coefficients [*Mlawer et al.*, 1997]

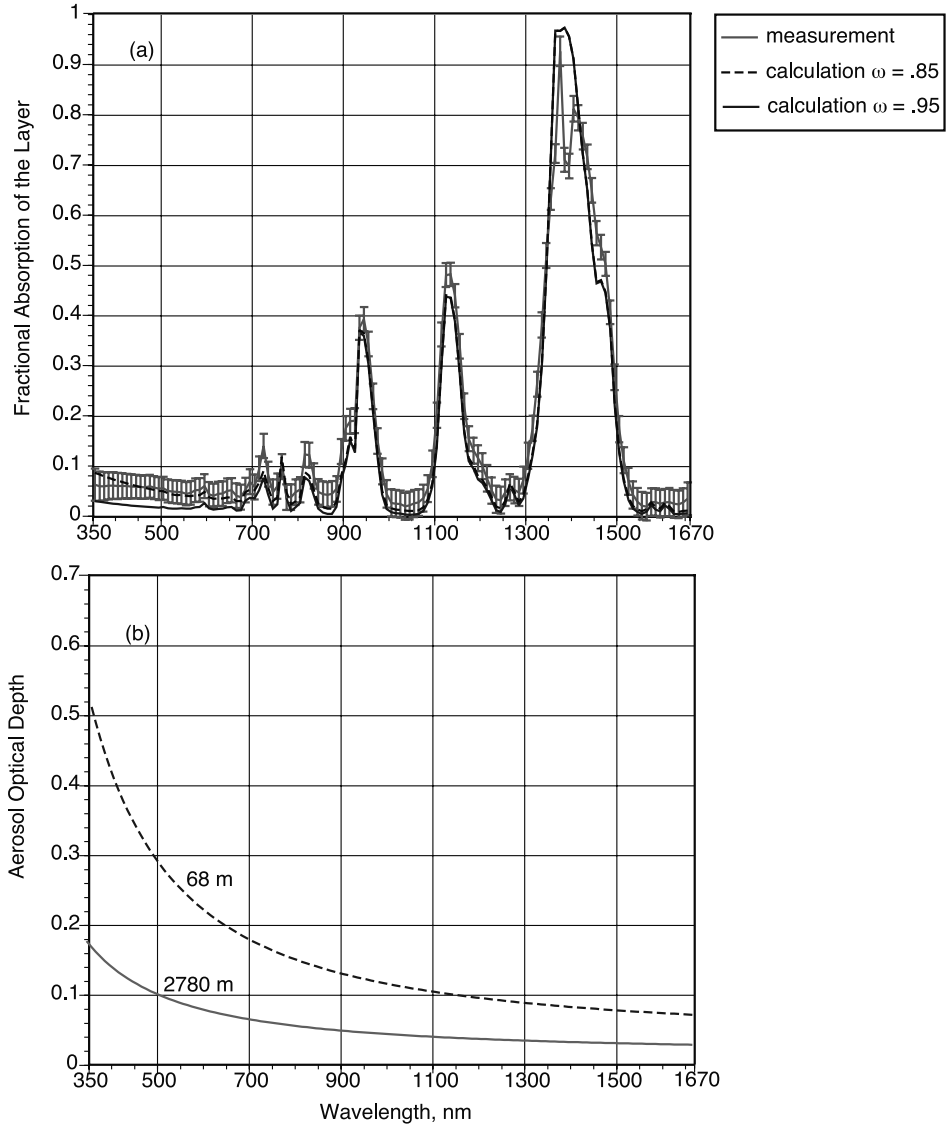

Figure 3. 24 August: Measured fractional absorption and calculated fractional absorption for two values of the single scattering albedo (a), optical depth at top and bottom of the aerosol layer (b).

2. DISORT, a multiple scattering code [*Stamnes et al.*, 1988]

3. Kurucz representation of the solar spectrum [*Kurucz*, 1992]

4. Filter functions from the SSFR [*Pilewskie et al.*, 2003]

[13] The model contains 140 bands of 10 nm width from 300 to 1700 nm matching the spectral coverage of the SSFR. The inputs are the vertical profiles of the gases, aerosol and clouds; as well as the spectral scattering and absorption properties of the aerosols and clouds. The spectral surface reflectance and the solar angle are also inputs. We simplify the aerosol scattering by assuming a Henyey-Greenstein phase function. This required specifying only the first moment of the phase function, the asymmetry parameter, g.

[14] The *k*-distribution technique has been discussed a number of times [e.g., *Goody and Yung*, 1989; *Mlawer et al.*, 1997] and is an effective method for treating the line absorption of atmospheric gases. The significance of the *k*-distribution technique is that it also allows for the accurate inclusion of scattering and absorption of gases and aerosols at a saving of several orders of magnitude computational effort compared to a line-by-line calculation.

[15] The line-by-line code LBLRTM (available on the LBLRTM web site, http://atmos.umd.edu/~bobe/LBLRTM) [*Clough and Iacono*, 1995] was used to compute the gas absorption coefficients at a resolution of 0.001 cm^{-1} from the HITRAN 1996 database [*Rothman et al.*, 1997] with the Giver corrections [*Giver et al.*, 2000]. At this resolution there are roughly 10^7 wave number intervals for the solar spectrum discussed here. The absorption coefficients for the gases were computed at 30 pressures from 1100 to 0.1 mb (in log pressure spacing) and at five temperatures at each pressure (±15° and ±30° from the model atmosphere) [*Mlawer et al.*, 1997]. This resulted in approximately 10^9 absorption coefficient calculations.

[16] For each 10-nm band and each temperature and pressure combination the coefficients were then sorted in cumulative probability space. Sixteen Gaussian quadrature points were used to compute the 16 absorption coefficient

values actually used (for more details, see *Mlawer et al.* [1997]). For each pressure and temperature in the atmosphere, the absorption coefficient values were interpolated (linear in temperature and logarithmically in pressure). The H_2O/CO_2 and H_2O/O_2 overlap was included. This requires defining the ratio of the overlapping gas amounts as an additional variable [*Mlawer et al.*, 1997] and then an interpolation in that ratio. Since both the solar source function and the gaseous absorption coefficients have a fine structure at a resolution of 0.001 cm^{-1}, it is necessary to account for the correlation between them. That is, to accurately integrate over a spectral interval, the pairing of absorption coefficient and solar source function must be maintained. The same requirement holds for the instrument filter functions.

[17] As an illustration of the spectral resolution of the model, Figure 1 shows the calculated direct transmitted solar beam for a midlatitude summer atmospheric profile. The figure illustrates the Kurucz solar spectrum attenuated by Rayleigh scattering, O_2, O_3 absorption in the UV, the O_2 A and B bands centered at 762 and 688 nm, the H_2O bands centered at 1380, 1135, and 942 nm as well as the visible H_2O bands, and the CO_2 bands at 1400 and 1600 nm.

3. Determining the Aerosol Single Scattering Albedo

[18] The fractional absorption, α, of the aerosol layer is related to the single scattering albedo, ω (the ratio of scattering to extinction), as [*Chandrasekhar*, 1960]

$$\alpha = \int_{\Delta\tau} (1-\omega)\left[\int_{4\pi} I(\tau,\Omega)/F_{\downarrow_2} d\Omega\right] d\tau \qquad (1)$$

where I is the spectral intensity (or radiance), Ω is the solid angle and τ is the spectral optical thickness. The fractional absorption of an aerosol layer is defined as

$$\alpha = \frac{(F_\downarrow - F_\uparrow)_2 - (F_\downarrow - F_\uparrow)_1}{F_{\downarrow_2}}$$

where $F_\downarrow$ and $F_\uparrow$ are the downward and upward flux, respectively. The subscripts 1 and 2 denote the lower and upper levels (top and bottom) of the aerosol layer.

[19] Equation (1) indicates that the fractional absorption is proportional to the co-albedo (1-ω). Since the spectral intensity is integrated over all angles, the fractional absorption is only weakly dependent on the scattering distribution function (or asymmetry factor). Therefore, the fractional absorption can be used to estimate the spectral co-albedo.

[20] One of the primary goals of this study is to assess the accuracy of the determination of the single scattering albedo from the measurements of the flux divergence. In the limit of single scattering of the direct beam over a dark surface equation (1) reduces to:

$$\alpha \sim (1-\omega)\left[1 - e^{-\tau/\mu_o}\right]$$

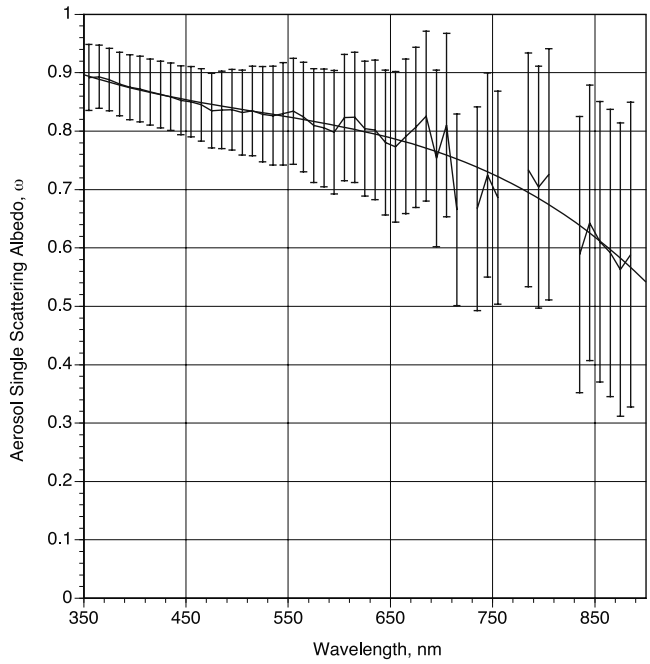

Figure 4. 24 August: Estimated single scattering albedo of the aerosol layer.

where μ_o is the cosine of the solar angle. Differentiating and solving for a change in the single scattering albedo with respect to a change in α and τ, we can write

$$\delta\omega = (1-\omega)\frac{\delta\alpha}{\alpha} + \frac{\left(1-\mu_o e^{-\tau/\mu o}\right)}{\left(1-e^{-\tau/\mu o}\right)}\delta\tau \qquad (2)$$

[21] From equation (2) we can estimate the uncertainty in the single scattering albedo from the uncertainty in the fractional absorption, α, and the uncertainty in the optical depth, τ.

[22] For the general case, the change in the single scattering albedo with respect to a change in α and τ is not analytic because of the integral in equation (1) is a function of the aerosol properties, the solar angle and the surface reflectance. As a practical matter, however, we can use equation (1) to get the error estimates in the single scattering albedo by computing the albedo for the upper and lower bounds of the fractional absorption and using the difference as the uncertainty in the single scattering albedo.

4. Case 1: 24 August 2000, Inhaca Island

[23] On 24 August 2000 the UW Convair 580 flew over the island off Inhaca of the coast of South Africa (latitude 26°S and longitude 33°E). The optical depth was relatively small as the flight was over the ocean away from the aerosol source regions. Data were taken during level passes at several heights between 60 and 2780 m. As inputs to the radiative transfer model, we used the aerosol optical depth from the AATS-14 measured on the aircraft, the surface reflectance from the SSFR measurements at the lowest altitude (60 m) and the ozone profile from the nearest ozone sondes (SHADOZ network). We obtained the water

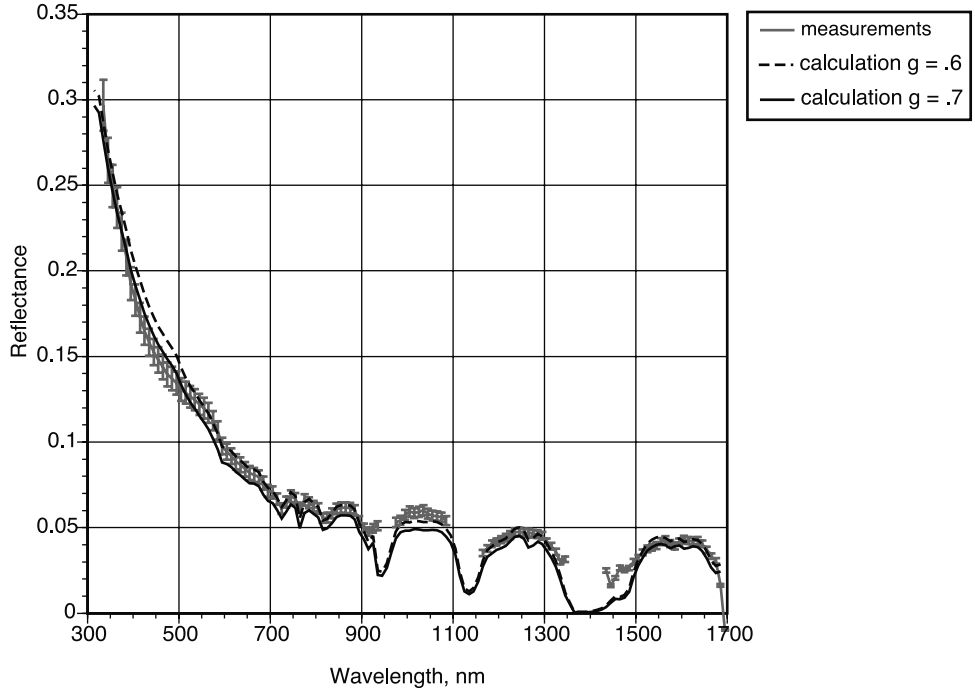

Figure 5. 24 August: Reflectance at the top of the aerosol layer, $\mu_0 = 0.80$.

vapor profile from the closest radiosondes and from the airborne Sun photometer [*Schmid et al.*, 2003] measurements. The cosine of the solar angle during the measurements was 0.80.

[24] Figure 2a shows the measured and computed downward flux at 2780 m. The residuals are shown in Figure 2b and are within the error estimates of *Pilewskie et al.* [2003] (~4%). The figure illustrates a slight misalignment of the 762-nm O_2 band and the larger percentage difference in the center of the 1380-nm water band where the irradiance is low. Also, the figure shows greater differences near the edges of the wavelength range of the SSFR.

[25] Figure 3 shows the measured fractional absorption in the layer between 68 and 2780 m. Also plotted is the calculated fractional absorption for two choices of constant single scattering albedo. The error bars in the fractional absorption are from *Pilewskie et al.* [2003] and are about 0.05 at 500 nm. This corresponds to about 40% uncertainty in the fractional absorption at 500 nm. The uncertainty becomes larger in the near infrared.

[26] The computed best fit single scattering albedo is shown in Figure 4 for the region of 350 to 900 nm. The calculation assumes an asymmetry factor of 0.6, see below. The error bars for the single scattering albedo are determined for the upper and lower bounds of the fractional absorption. We computed the single scattering albedo for the upper and lower bounds and used the difference as the error bar for the single scattering albedo. The calculated uncertainty was 0.073 at 500 nm.

[27] If we use the first term of the right-hand side of equation (2) above to estimate the uncertainty in the single scattering albedo given the uncertainty in the fractional absorption at 500 nm we get an uncertainty of 0.062. From the second term of the right-hand side of equation (2) the estimated uncertainty in the single scattering albedo due to the optical depth measurement (0.02) is 0.014. The sum of the two is 0.076 which is close to the uncertainty shown in Figure 4.

[28] As discussed above, there is very little dependence of the fractional absorption on the choice of the asymmetry factor. A change from 0.6 to 0.7 in the asymmetry factor resulted in a maximum change of 0.1% in the fractional absorption.

[29] After estimating the single scattering albedo from the fractional absorption, we can attempt to determine the asymmetry factor from the upward flux (reflectance) from the upper layer. Figure 5 shows the reflectance of the layer for the derived single scattering albedo and for two choices of asymmetry factor. As shown, the asymmetry factor is likely between 0.7 and 0.6, but both choices are within the error bars of the model and the measurements, except for regions dominated by water vapor absorption and an anomalous region around 400 nm.

5. Case 2: 6 September 2000, Mongu, Zambia

[30] On 6 September 2000 the UW Convair 580 flew over Mongu, Zambia. This day was part of the "river of smoke" period (H. Annegarn et al., "The river of smoke": Characteristics of the southern African springtime biomass burning haze, submitted to *Journal of Geophysical Research*, 2002.) and represented the largest optical thickness experienced by the Convair 580 (1.0 in the midvisible for the aerosol layer). The upper leg was at 4800 m and the lower leg was at 1200 m. Again, we used inputs of the aerosol optical depth from the NASA Ames Sun photometer on the UW Convair 580 [*Schmid et al.*, 2003], the surface reflectance from the SSFR measurements at the lowest altitudes and the ozone

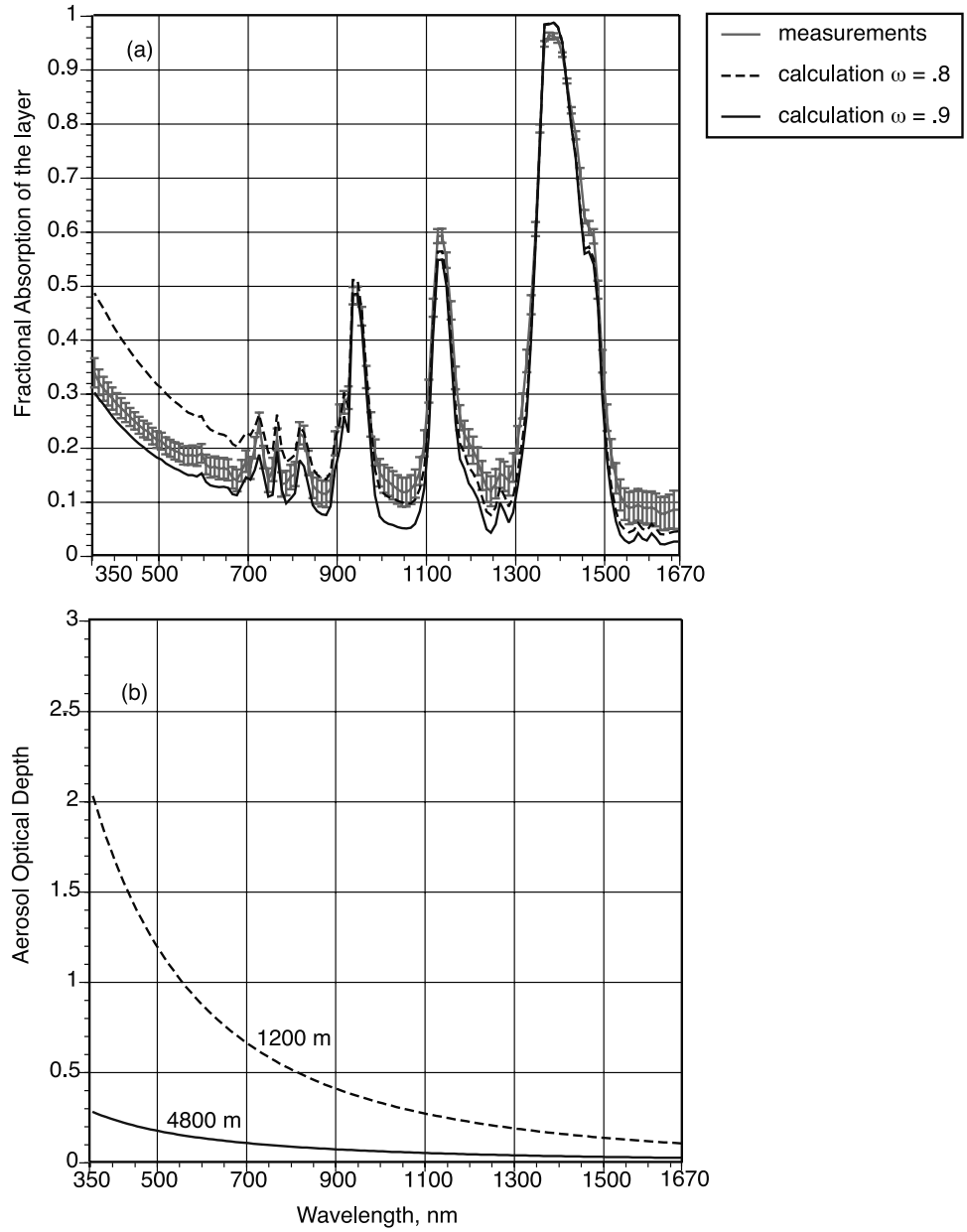

Figure 6. 6 September: Measured fractional absorption and calculated fractional absorption for two values of the single scattering albedo of the aerosol layer (a), aerosol optical depth of top and bottom of aerosol layer (b).

profile from ozonesondes (SHADOZ network). The water vapor profile was estimated from radiosondes and the airborne Sun photometer measurements of *Schmid et al.* [2003]. The cosine of the solar angle during the measurements was 0.89.

[31] The fractional absorption in the layer is shown in Figure 6 with the error bars placed on the measured values from *Pilewskie et al.* [2003]. The absorption can be bracketed in the visible between single scattering albedo values of 0.90 and 0.80 in the visible with the inferred single scattering albedo being less in the near infra-red.

[32] The computed best fit single scattering albedo is shown in Figure 7 with the wavelength regions dominated by gaseous absorption removed. Again, the estimated single scattering albedo is between 0.85 and 0.9 in the visible, decreasing to 0.6 in the near infrared. The spectral dependence and magnitude of the single scattering albedo for 24 August and 6 September are quite similar indicating that biomass burning dominated the aerosol sources, even in a relatively clean area. The estimated single scattering albedo at 500 nm on 24 August was 0.83 and on 6 September it was 0.89.

[33] The error bars for the single scattering albedo are again estimated by determining the single scattering albedos for the upper and lower bounds of the fractional absorption. In this case, the error bars are considerably smaller than those for the 24 August case (0.02 at 500 nm). This is due to the fact that the optical thickness of the layer and the fractional absorption on 6 September are four to five times are large as the optical thickness and fractional absorption

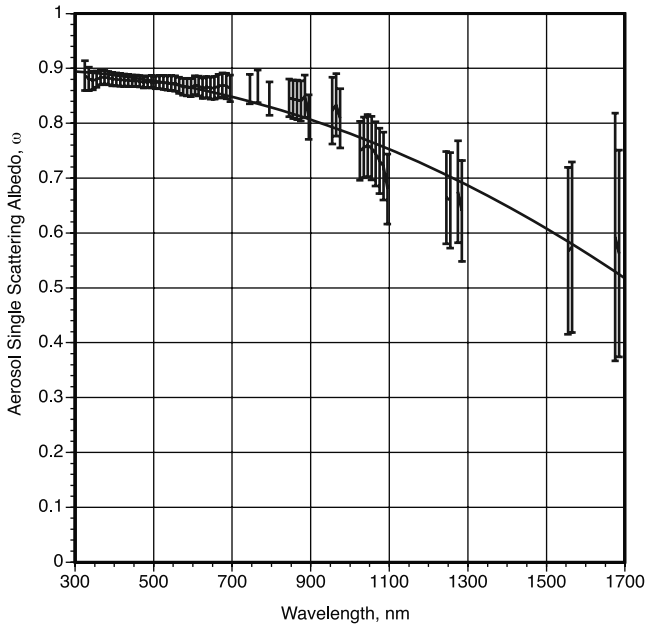

Figure 7. 6 September: Estimated single scattering albedo.

for 24 August. We fit a second-order polynomial to the estimated values of single scattering albedo and used those values in recomputing the fractional absorption shown in Figure 8. The second-order polynomial fit the data slightly better than a third-order polynomial.

[34] As mentioned above, the decreasing single scattering albedo with wavelength in Figure 4 and Figure 7 is characteristic of the absorption by small elemental carbon particles in a mixture of nonabsorbing particles as discussed by *Bergstrom et al.* [2002]. The decrease results from the absorption coefficient having a weaker wavelength dependence than the scattering coefficient. The magnitude of the single scattering albedo in the visible agrees with several other estimates for African biomass burning [*Dubovik et al.*, 2002; *Eck et al.*, 2001]. The magnitude and wavelength dependence also agree well with other SAFARI 2000 investigators [*Eck et al.*, 2003; *Haywood et al.*, 2003; B. I. Magi et al., Vertical profiles of light scattering, light absorption and single scattering albedo during the dry, biomass burning season in southern Africa and comparisons of in situ and remote sensing measurements of aerosol optical depths, submitted to *Journal of Geophysical Research*, 2002].

[35] *Dubovik et al.* [1998] inferred the aerosol absorption optical depth from sky radiance data for areas that have significant biomass burning. Their results show that for one year the wavelength dependence was λ^{-1} but for two other years the wavelength dependence was greater than λ^{-2}. *Bergstrom et al.* [2002] reported a roughly λ^{-1} decrease in the absorption coefficient with wavelength based on the data from the TARFOX field experiment conducted off the Eastern coast of the U.S. For the 24 August case, the fall off in the aerosol absorption coefficient is approximately λ^{-1}. However, the error bars are rather large. For the 6 September case, the estimated absorption coefficient has an approximate λ^{-2} decrease with wavelength in the visible and a λ^{-1} (with large error bars) in the near IR. This faster falloff agrees with *Bond* [2001] results from coal combustion and some of *Dubovik et al.* [1998] results.

[36] The aerosol optical depth of the layer sampled on 6 September was large enough that even for a small co-albedo ($1 - \omega$), the fractional absorption is significant. Figure 9 shows the absorption for single scattering albedos of 0.99 and 0.999. Even for a single scattering albedo of 0.99 the predicted absorption in the visible is about 3–5%.

[37] We can estimate the aerosol asymmetry factor from the layer reflectance, Figure 10. These results indicate an asymmetry factor of 0.8 at 350 nm to 0.6 at 700 nm. The asymmetry factor usually decreases with wavelength as the particles become smaller with respect of the wavelength of the solar radiation. However, in the near infrared the model appears to underpredict the reflection making the inferred asymmetry factor unrealistic.

[38] We can also estimate the amount of water in the layer from the fractional absorption in the water bands. We estimate an amount of 1.2 cm for the 6 September case. This is slightly larger than the amount of 1.0 cm determined by *Schmid et al.* [2003] who used the transmission of the 942 nm water vapor band. However, *Schmid et al.* [2003] used different water line strengths instead of the HITRAN 1996 with the Giver corrections that may explain much of the difference.

6. Estimation of the Aerosol Effects on the Solar Radiation

[39] By removing the aerosol from the calculations and comparing the results with the results that include aerosols, we can estimate the effect of the aerosol on the solar fluxes. We define the effect of the aerosol at the top of the atmosphere (TOA) as the difference between the net flux (downward flux minus upward flux) with aerosol and the net flux without aerosol. In this convention, a positive change in the net flux is heating and a negative change is

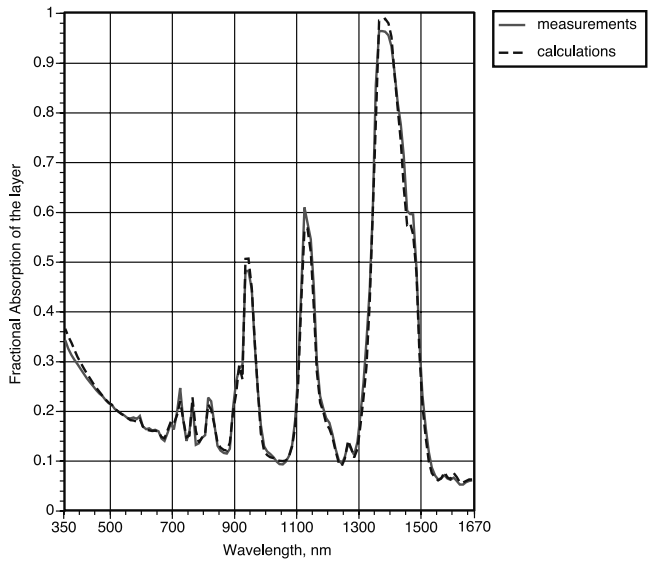

Figure 8. 6 September: Calculated fractional absorption using derived value of the single scattering albedo.

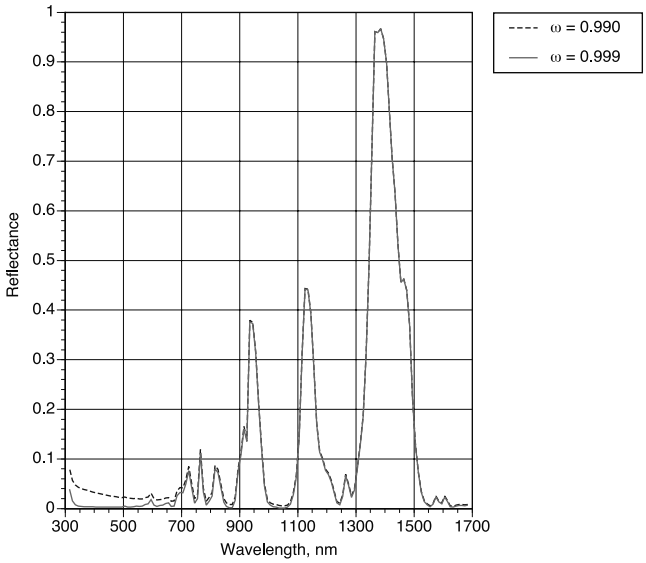

Figure 9. 6 September: Fractional absorption for high values of the single scattering albedo.

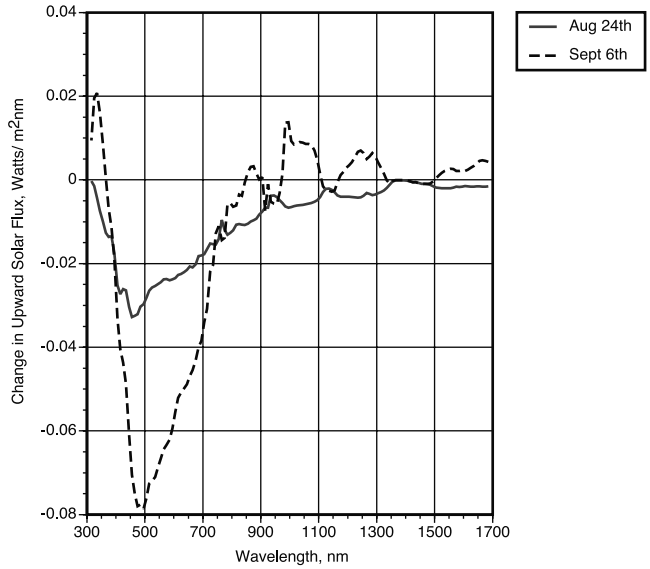

Figure 11. Computed effect of the aerosol on upward flux at TOA.

cooling. The results of the computations are shown in Figure 11 for the change in the net flux at the TOA for both days.

[40] At the TOA, the 24 August case results in a cooling of the Earth-atmosphere system at all wavelengths. The spectrally integrated TOA net flux change is -13 W m^{-2}. The results for 6 September are somewhat different. The aerosol actually reduces the upward flux (increases the net flux) in the 300- to 360-nm region. This reduction is caused by absorption and the fact that the aerosol has much less backscattering than Rayleigh scattering (which has $g = 0$). This effect is utilized by the Total Ozone Mapping Spectrometer (TOMS) satellite sensor and is used to derive an "Aerosol Index" [*Hsu et al.*, 1999]. A positive Aerosol Index means that the aerosol reduces the upward reflection due to Rayleigh scatter. The TOMS data for 6 September (available on the TOMS website) shows a region of positive Aerosol Index over parts of southern Africa including the latitude and longitude of Mongu consistent with our calculations.

[41] In the visible, the aerosol cooling effect at the TOA is larger on 6 September than on 24 August.

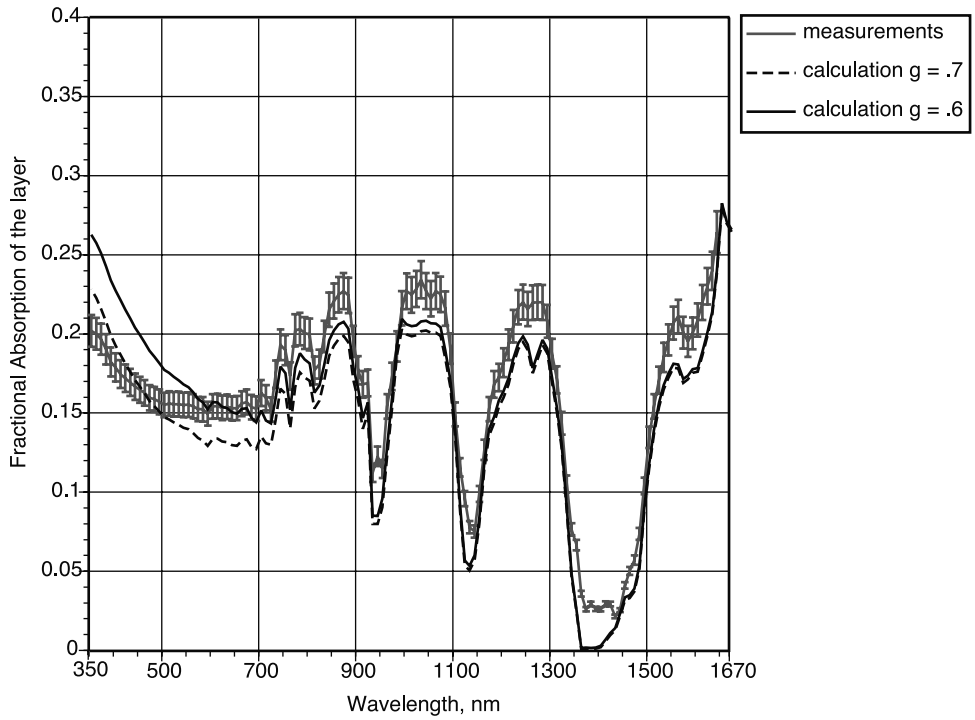

Figure 10. 6 September: Upward reflectance at the top of the aerosol layer, $\mu_0 = 0.89$.

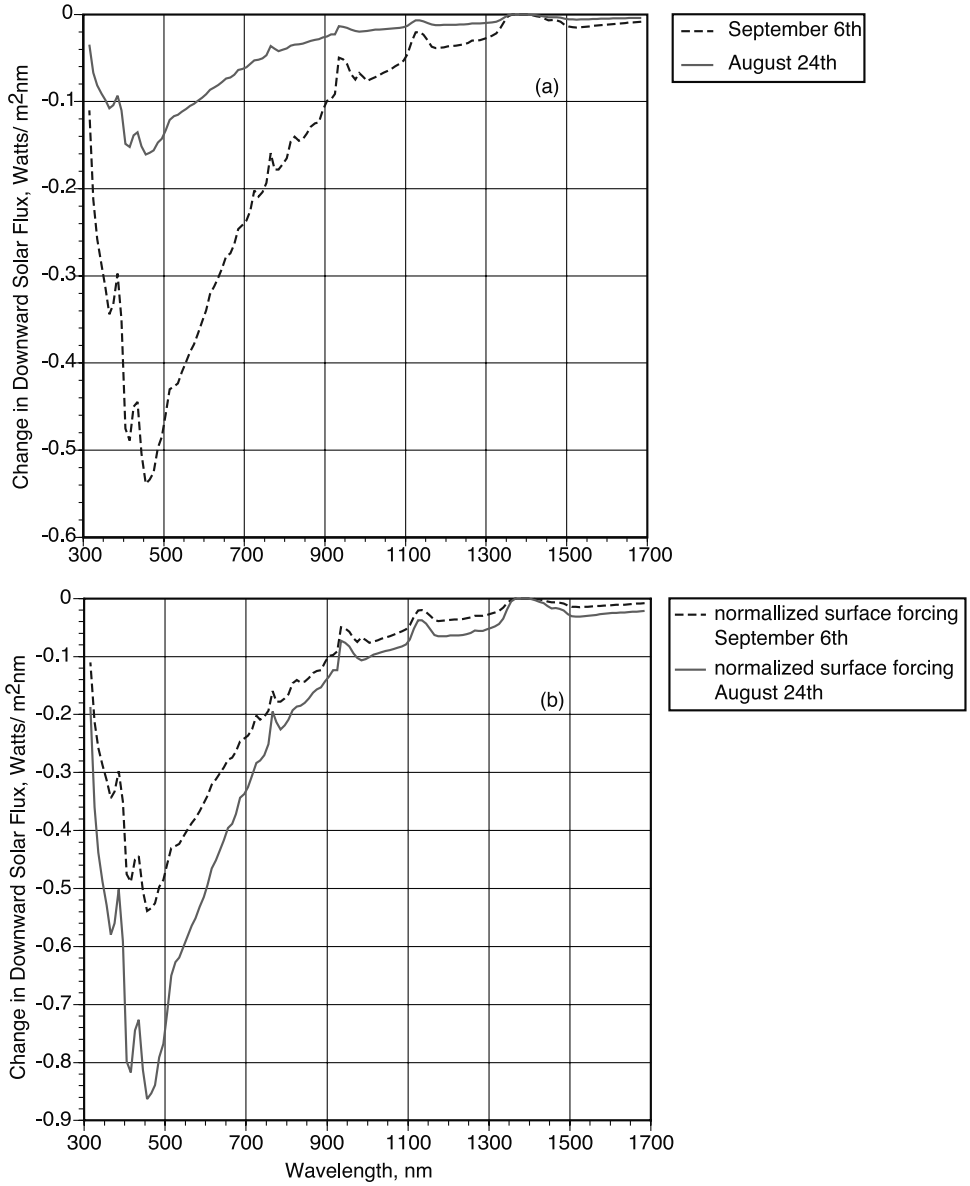

Figure 12. Computed effect of aerosol on the downward flux at surface (a) and the effect normalized by the optical depth of the layer at 500 nm (b).

Considering that the optical depth on 6 September was about 5 times the optical depth, the cooling in the visible is very similar on the 2 days. The surface albedo of Mongu was very low and similar to the ocean surface. In the near IR the aerosol actually warms the Earth-atmosphere system on 6 September as the land surface albedo is higher than in the visible. The spectrally integrated amount of net aerosol effect is about -17 W m^{-2} on 6 September.

[42] The computed effect of the aerosols on the downward flux at the surface is shown in Figure 12a for both days. Here to facilitate comparison to the INDOEX results we define the aerosol effect as the downward flux with aerosol minus the downward flux without aerosol. At the surface, the aerosol can only reduce the downward flux so that the effect is always negative. On both days the aerosol reduces the surface flux considerably and the spectral shape is very similar. The spectrally integrated change in the downward flux is about -57 W m^{-2} on 24 August and -208 W m^{-2} on 6 September. Figure 12b shows the surface forcing normalized by the aerosol optical depth at 500 nm. As shown, the normalized surface forcing on the lower optical depth day (24 August) is larger than the high-optical-depth day since the surface forcing is not linear in optical depth over this range of optical depth. However, *Pilewskie et al.* [2003] show that the aerosol absorption efficiency (absorption per optical depth) of the two days is almost identical.

[43] *Meywerk and Ramanathan* [1999] measured the downward spectral solar flux at the surface during INDOEX and computed the aerosol effect. They estimated a maximum of 0.6 W m^{-2} nm^{-1} at 450 nm for an aerosol optical depth at 500 nm of 1.0 [*Meywerk and Ramanathan*, 1999, Plate 5]. We estimate 0.55 W m^{-2} nm^{-1} at 450 nm (Figure

12a) for the analogous quantity on 6 September during SAFARI 2000. Also, the spectral shape of the effect is quite similar to that reported by *Meywerk and Ramanathan* [1999].

7. Summary

[44] Using the fractional absorption and the aerosol layer optical depth measured on the same aircraft during SAFARI 2000, we estimate the magnitude and uncertainty of the aerosol single scattering albedo for 2 days. The aerosol single scattering albedo is between 0.85 and 0.9 at 350 nm and decreases with wavelength. The spectral behavior is indicative of the absorption by small elemental carbon particles and the steeper wavelength dependence of the particle scattering relative to absorption.

[45] The aerosol radiative effect was computed at the top of the atmosphere (defined as the difference in the net flux) and on the downward flux at the surface. The estimated TOA effect was to increase the upward flux (cooling) by 13 W m^{-2} on 24 August and 17 W m^{-2} on 6 September. The aerosol effect on the downwelling flux at the surface was 57 W m^{-2} on 24 August and 208 W m^{-2} on 6 September. As the spectral shape was similar on both days the differences were due to the higher optical depth on 6 September.

[46] **Acknowledgments.** This research was supported by the Radiation Science Program Office and the Earth Observing System Inter-Disciplinary Science (EOS-IDS) Program of the U.S. National Aeronautics and Space Administration. The contributions of Eli Mlawer and Tony Clough of AER, Inc. are greatly appreciated. This research was conducted as part of the Southern African Regional Science Initiative (SAFARI 2000).

References

Ackerman, A. S., O. B. Toon, D. E. Stevens, A. J. Heymsfield, V. Ramanathan, and E. J. Welton, Reduction of tropical cloudiness by soot, *Science*, *288*, 1042–1047, 2000.

Bergstrom, R. W., P. B. Russell, and P. Hignett, The wavelength dependence of black carbon particles: Predictions and results from the TARFOX experiment and implications for the aerosol single scattering albedo, *J. Atmos. Sci*, *59*, 567–577, 2002.

Bond, T. C., Spectral dependence of visible light absorption by carbonaceous particles emitted from coal combustion, *Geophys. Res. Lett.*, *28*, 4075–4078, 2001.

Chandrasekhar, *Radiative Transfer*, 393 pp., McGraw-Hill, New York, 1960.

Clough, S. A., and J. M. Iacono, Line-by-line calculations of atmospheric fluxes and cooling rates, 2, Application to carbon dioxide, ozone methane, nitrous oxide and the halocarbons, *J. Geophys. Res.*, *100*, 16,519–16,535, 1995.

Dubovik, O., B. N. Holben, Y. J. Kaufman, M. Yamasoe, A. Smirnov, D. Tanre, and I. Slutsker, Single scattering albedo of smoke retrieved from the sky radiance and solar transmittance measured from ground, *J. Geophys. Res.*, *103*, 31,903–31,923, 1998.

Dubovik, O., B. Holben, T. F. Eck, A. Smirnov, Y. Kaufman, M. D. King, D. Tanre, and I. Slutsker, Variability of absorption and optical properties of key aerosol types observed in worldwide locations, *J. Atmos. Sci.*, *59*, 590–608, 2002.

Eck, T. F., B. N. Holben, D. E. Ward, O. Dubovik, J. S. Reid, A. Smirnov, M. M. Mukelabai, N. C. Hsu, N. T. O'Neil, and I. Slusker, Characterization of the optical properties of biomass burning aerosol in Zambia during 1997 the ZIBBEE field campaign, *J. Geophys. Res.*, *106*, 3425–3448, 2001.

Eck, T., et al., Variability of biomass burning aerosol optical characteristics in southern Africa during the SAFARI 2000 dry season campaign and a comparison of single scattering albedo estimates from radiometric measurements, *J. Geophys. Res.*, *108*, doi:10.1029/2002JD002321, in press, 2003.

Giver, L. P., C. Chackerian, and P. Varanasi, Visible and near-infrared $H_2{}^{16}O$ line intensity corrections for HITRAN-96, *J. Quant. Spectrosc. Radiat. Transfer*, *66*, 101–105, 2000.

Goody, R. M., and Y. L. Yung, *Atmospheric Radiation, Theoretical Basis*, 2nd ed., 519 pp., Oxford Univ. Press, New York, 1989.

Haywood, J. M., P. N. Francis, M. D. Glew, O. Dubovik, and B. Holben, Comparison of aerosol size distributions, radiative properties and optical depths determined by aircraft observations and sunphotometers during SAFARI-2000, *J. Geophys. Res.*, *108*, doi:10.1029/2002JD002250, in press, 2003.

Heintzenberg, J., R. J. Charlson, A. D. Clarke, C. Liousse, V. Ramaswamy, K. P. Shine, M. Wendish, and G. Helas, Measurements and modelling of aerosol single scattering albedo: Progress, problems and prospects, *Beitr. Phys. Atmos.*, *70*, 249–263, 1997.

Hsu, N. C., J. R. Herman, O. Torres, B. N. Holben, D. Tanre, T. F. Eck, A. Smirnov, B. Chatenet, and F. Lavenu, Comparisons of the TOMS aerosol index with Sun-photometer aerosol optical thickness: Results and applications, *J. Geophys. Res.*, *105*, 6269–6279, 1999.

Kurucz, R. L., Synthetic infrared spectra, in *Infrared Solar Physics*, *IAU Symp.*, vol. 154, edited by D. M. Rabin and J. T. Jeffries, Kluwer, Norwell, Mass, 1992. (Available on the LBLRTM web site)

Mlawer, E. J., S. J. Taubman, P. D. Brown, M. J. Iacono, and S. A. Clough, Radiative transfer for inhomogeneous atmospheres: RRTM, a validated correlated-k model for the longwave, *J. Geophys. Res.*, *102*, 4353–4356, 1997.

Meywerk, J., and V. Ramanathan, Observations of the spectral clear-sky aerosol forcing over the tropical Indian Ocean, *J. Geophys. Res.*, *104*, 24,359–24,370, 1999.

Pilewskie, P., J. Pommier, R. Bergstrom, W. Gore, M. Rabbette, S. Howard, B. Schmid, and P. V. Hobbs, Solar spectral radiative forcing during the Southern African Regional Science Initiative, *J. Geophys. Res.*, *108*, doi:10.1029/2002JD002411, in press 2003.

Ramanathan, V., T. S. Bates, J. E. Hansen, D. J. Jacob, Y. J. Kaufman, J. E. Penner, M. J. Prather, S. E. Schwartz, and J. H. Seinfeld, National Aerosol-Climate Interactions Program (NACIP), A National Research Imperative, white paper, 11 pp., 2002.

Reid, J. S., and P. V. Hobbs, Physical and optical properties of young smoke from individual biomass fires in Brazil, *J. Geophys. Res.*, *103*, 32,013–32,030, 1998.

Russell, P. B., et al., Comparison of aerosol single scattering albedos derived by diverse techniques in two North Atlantic experiments, *J. Atmos. Sci.*, *59*(3), 609–619, 2002.

Rothman, L. S., et al., The 1996 HITRAN Molecular Spectroscopic Database and HAWKS (HITRAN Atmospheric Workstation), *J. Quant. Spectrosc. Radiat. Transfer*, *60*(5), 665–710, 1997.

Schmid, B., et al., Coordinated airborne, spaceborne, and ground-based measurements of massive, thick aerosol layers during the dry season in southern Africa, *J. Geophys. Res.*, *108*, doi:10.1029/2002JD002297, in press, 2003.

Sinha, P., P. V. Hobbs, R. J. Yokelson, I. Bertschi, D. R. Blake, I. J. Simpson, S. Gao, T. L. Kirchstetter, and T. Novakov, Emissions of trace gases and particles from savanna fires in southern Africa, *J. Geophys. Res.*, *108*, doi:10.1029/2002JD002325, in press, 2003.

Stamnes, K., S.-C. Tsay, W. Wiscombe, and K. Jayaweera, A numerically stable algorithm for discrete-ordinate-method radiative transfer in multiple scattering and emitting layered media, *Appl. Opt.*, *27*, 2502–2509, 1988.

Swap, R. J., et al., The Southern African Regional Science Initiative (SAFARI 2000): Dry season field campaign: An overview, *S. Afr. J. Sci.*, *98*, 126–130, 2002.

R. W. Bergstrom and B. Schmid, Bay Area Environmental Research Institute, Sonoma, CA 95476-6502, USA. (bergstro@sky.arc.nasa.gov)

P. Pilewskie and P. B. Russell, NASA Ames Research Center, Moffett Field, CA 94035-1000, USA.